AKAP9 regulation of microtubule dynamics promotes Epac1-induced endothelial barrier properties

*Seema Sehrawat,[1] *Thomas Ernandez,[1] Xavier Cullere,[1] Mikiko Takahashi,[2] Yoshitaka Ono,[2] Yulia Komarova,[3] and Tanya N. Mayadas[1]

[1]Center for Excellence in Vascular Biology, Department of Pathology, Brigham and Women's Hospital and Harvard Medical School, Boston, MA; [2]Biosignal Research Center, Kobe University, Kobe, Japan; and [3]Department of Pharmacology and Center for Lung and Vascular Biology, University of Illinois College of Medicine, Chicago, IL

Adhesive forces at endothelial cell-cell borders maintain vascular integrity. cAMP enhances barrier properties and controls cellular processes through protein kinase A bound to A-kinase anchoring proteins (AKAPs). It also activates exchange protein directly activated by cAMP (Epac1), an exchange factor for Ras-related protein 1 (Rap1) GTPases that promotes cadherin- and integrin-mediated adhesion through effects on the actin cytoskeleton. We demonstrate that AKAP9 facilitates the microtubule polymerization rate in endothelial cells, interacts with Epac1, and is required for Epac1-stimulated microtubule growth. AKAP9 is not required for maintaining barrier properties under steady-state conditions. Rather, it is essential when the cell is challenged to make new adhesive contacts, as is the case when Epac activation enhances barrier function through a mechanism that, surprisingly, requires integrin adhesion at cell-cell contacts. In the present study, defects in Epac-induced responses in AKAP9-silenced cells were evident despite an intact Epac-induced increase in Rap activation, cortical actin, and vascular endothelial-cadherin adhesion. We describe a pathway that integrates Epac-mediated signals with AKAP9-dependent microtubule dynamics to coordinate integrins at lateral borders. (*Blood*. 2011;117(2): 708-718)

Introduction

Adherens junctions (AJs) at endothelial cell-cell contacts regulate the barrier properties of the endothelium by controlling the infiltration of plasma components and cells into the tissue. They undergo continuous remodeling in resting monolayers and in response to agents that alter permeability. These events are primarily coordinated by vascular endothelial (VE) cadherin and its associated cytoplasmic proteins, cytoskeletal-based contractile forces, and small GTPases.[1] Endothelial integrins promote cell adhesion, spreading, migration, and survival, and, in concert with AJs, also contribute to barrier integrity.[2,3] Although well known to bind at the cell-matrix interface, integrins also localize to endothelial junctions, where they may regulate barrier properties.[4]

cAMP is a well-known secondary messenger that enhances barrier properties, and its principal target is protein kinase A (PKA), which increases barrier function by reducing actomyosin contractility.[2] PKA interacts with A-kinase anchoring proteins (AKAPs), a family of scaffolding proteins that reside in certain subcellular sites to spatially and temporally compartmentalize cAMP signaling.[5] In addition, cAMP activates exchange protein directly activated by cAMP (Epac) proteins, which are guanine exchange factors for Ras-related protein 1 (Rap) GTPases that, in limited cases, transduce their signals by interacting with AKAP complexes.[6,7] Epacs regulate several cellular functions, ranging from cell-cell and cell-matrix interactions, exocytosis, and cellular Ca^{2+} handling to gene expression.[8] In endothelial cells (ECs), Epac1 activation enhances barrier function by increasing VE-cadherin adhesion and cortical actin, and opposes the effects of edemagenic agents and Rho GTPase activation.[8] Recent work suggests that Epac interacts with microtubules (MTs) and the microtubule binding protein MAP1A,[9,10] and enhances microtubule growth in ECs.[11]

Many aspects of cell-cell and cell-matrix adhesion require reorganization of actin and MTs at cortical sites. In contrast to the well-described relationship between cadherins and integrins with the actin cytoskeleton, the role of MTs in regulating these complexes is only beginning to be elucidated.[12] MTs are highly dynamic structures. Commonly, the minus ends of MTs anchor at the centrosome and Golgi, while the plus ends establish transient interactions with sites of cell-to-cell and focal adhesions. This facilitates the delivery of cargo to maintain a gradient of AJ components and induces the turnover of focal adhesions. Microtubule dynamics, microtubule linkage to actin, and their capture at cortical sites are regulated by plus-end-binding proteins (+TIPs) such as EB1, CLIP-170, and CLASPs, which transiently bind to the plus ends of growing MTs.[13] There is evidence that AKAP9 participates in microtubule remodeling. AKAP9 exists as both long isoforms and a short isoform called Yotiao.[14] The long isoforms (350-450 kDa) localize to the centrosome and Golgi in interphase cells and promote microtubule regrowth,[15] and recent studies have shown that they confer microtubule nucleating activity at the Golgi.[16] However, the contribution of AKAP9 to the regulation of microtubule dynamics is not well understood, and the biological

Submitted February 5, 2010; accepted October 4, 2010. Prepublished online as *Blood* First Edition paper, October 15, 2010; DOI: 10.1182/blood-2010-02-268870.

The online version of this article contains a data supplement.

The publication costs of this article were defrayed in part by page charge payment. Therefore, and solely to indicate this fact, this article is hereby marked "advertisement" in accordance with 18 USC section 1734.

*S.S. and T.E. contributed equally to this study.

role of these large isoforms in cellular responses remains largely unexplored. We tested the hypothesis that AKAP9 and Epac1 interact functionally to enhance the barrier properties of the endothelium through effects on microtubule dynamics.

Methods

Antibodies and reagents

Rabbit anti-AKAP9[17] was a gift from Drs Lei Chen and Robert Kass (Columbia University, New York, NY); anti-dynein light chain[18] was a gift from Kerry S. Campbell (Fox Chase Cancer Center, Philadelphia, PA); and anti-Glu tubulin[19] was a gift from Dr G. G. Gunderson (Columbia University). Antibodies obtained from commercial sources were: VE-cadherin (Beckman Coulter); EB1 and GM130 (BD Biosciences); γ-tubulin (Abcam); integrin $\alpha_V\beta_3$ (CD51/61) and $\alpha_5\beta_1$ (CD94e; Chemicon); Yotiao (Invitrogen); platelet-endothelial cell adhesion molecule-1 (PECAM-1), β-catenin, and p-120 (BD Biosciences); Rap1 (Santa Cruz Biotechnology); flag (mouse monoclonal, clone M2), α-tubulin, V5, and β-actin (Sigma-Aldrich); pericentrin (Covance); and Epac1 (Cell Signaling Technology). The reagents fibronectin, collagen type IV, phalloidin, nocodazole, RGD (Arg-Gly-Asp), RGE (Arg-Gly-Glu) peptide, and 4,6-diamidino-2-phenylindole (DAPI) were from Sigma-Aldrich; hVE-Cadherin-Fc was from R&D Systems; sphingosine-1-phosphate (S1P) was from Calbiochem; and 8-pCPT-2′*O*-Me-cAMP (O-Me-cAMP) and N6-Benzolyadenosine-3′,5′-cyclic monophosphate (6-Benz-cAMP) were from BIOLOG Life Science Institute.

Plasmid and virus production

Green fluorescent protein (GFP)–end-binding protein 1 (EB1) cDNA[20] was used to generate adenovirus using the ViraPower Adenoviral Expression System (Invitrogen). Flag-AKAP9$^{2875\text{-}3899}$, AKAP9$^{1917\text{-}2876}$, AKAP9$^{1229\text{-}1917}$, and AKAP9$^{16\text{-}1229}$ plasmids were as described previously,[21] and empty CMV-3Xflag14 vector was from Sigma-Aldrich. The Epac1-V5 and the Epac1-flag constructs were generated by PCR using the Epac1-YFP cDNA[22] provided by Dr Xiaodong Cheng (University of Texas, Galveston, TX).

Cell culture, RNA interference, and gene delivery

Human umbilical vein endothelial cells (HUVECs) were isolated and cultured on fibronectin-coated dishes. All endothelial experiments were conducted on HUVECs except where indicated. Human dermal microvascular endothelial cells (HDMECs) were a kind gift from Dr A. Kowalczyk (Emory University, Atlanta, GA). Cells were seeded onto fibronectin (5 μg/mL)–coated glass coverslips for immunofluoresence studies, and onto fibronectin (5 μg/mL) or collagen (0.8 mg/mL) gold-coated microelectrodes for electrical resistance measurements. Cells were treated as follows: 100μM O-Me-cAMP, 200μM 6-Benz cAMP, 1μM S1P, 800μM RGD, 800μM RGE, 30 μg/mL anti-α_5, or 30 μg/mL anti-$\alpha_v\beta_3$ for functional blocking studies. ECs were electroporated with 600nM AllStars Negative Control small interfering RNA (siRNA; QIAGEN) or AKAP9- or Epac1-specific siRNA duplexes (QIAGEN) using Nucleofector (Amaxa Biosystems). AKAP9 siRNA sequences were as follows: AKAP9_4, 5′-CAGGTTCGTGAATATATGGAA-3′, AKAP9_5, 5′-CAGCCTATCAGTGAACATCAA-3′. The Epac1 siRNA sequence was Hs_RAPGEF3_2 5′-AGGGCACTTCGTGGTACATTA-3′. The siRNA-transfected cells were examined after 48 hours. For live-cell imaging, HUVECs transfected with siRNA were infected with EB1-GFP–expressing adenovirus. AKAP9 and Epac1-tagged plasmids were transfected into HEK 293T cells using Lipofectamine 2000 (Invitrogen).

Quantitative reverse transcriptase–PCR

RNA was isolated, cDNA was synthesized, and validated primer sets for GAPDH (QT0119264), AKAP9(350/450) (QT00090454), and Yotiao (QT01014069; all from QIAGEN) were used in real-time PCR assays performed on a StepOnePlus instrument (Applied Biosystems) using SYBR Green (Fermentas). Data were analyzed using the $2^{-\Delta\Delta Ct}$ method normalizing for GAPDH expression as an internal control.[23] Results were expressed as a percentage of control (set at 100%).

Microtubule regrowth assay and quantification of microtubule length

MTs were depolymerized on ice with 5μM nocodazole for 1 hour. Regrowth was induced by incubation in prewarmed medium (37°C) in the presence or absence of 100μM O-Me-cAMP. Cells were stained with anti–α-tubulin antibody and counterstained with DAPI (to visualize nuclei). Images were captured using a Nikon Eclipse TE2000-U camera with a 20× lens. Collected data were processed using Photoshop software (Adobe Systems). Net changes in microtubule length were analyzed using the neurite extension application from MetaMorph software Version 7.1 (Molecular Devices).[24] Analysis was performed on 8 to 10 randomly chosen fields per group, as described previously.[11]

Immunofluorescence microscopy, immunohistochemistry, and live cell imaging

For immunofluorescence analysis, HUVECs were plated on fibronectin- or collagen-coated glass coverslips (Fisher). Epifluorescence imaging of fixed samples and live cell imaging were conducted on a Nikon Eclipse TE-2000U inverted microscope using a 60× Plan Apo oil-immersion objective and a Himamatsu Photonics, ORCA-AG high-resolution digital camera (model: C4742-80-12AG). For live cell imaging, HUVECs were cultured on FN-coated glass-bottom MatTEK plates (MatTEK Corp) in M199 HUVEC medium without phenol red, the media was covered with mineral oil, and cells were imaged at 37°C. Confocal images were obtained with an Olympus BX50WI microscope with a 60× objective. The acquisition and analysis software was MetaMorph (Molecular Devices). Immunohistochemistry was performed on OCT-embedded human skin sections using a 2-layer peroxidase method. Samples were stained with anti-Yotiao (also recognizing AKAP350/450) and anti–PECAM-1 and counterstained with Gill Hematoxylin No. 2 (Fisher). Images were taken on a Nikon Microphot-FXA using a 10× objective.

Analysis of microtubule dynamics

The following parameters of microtubule dynamics were determined: instantaneous rates of growth, growth length, number of growing microtubule ends along the cell radius, and frequency of catastrophe events, as described previously.[25] Briefly, live cell images were collected every 3 seconds for 50-60 frames. Data analysis was performed on 16-bit images using MetaMorph software. The length of growth from the centrosome was measured for individual MTs, and the life histories of MTs were plotted as length (in micrometers) versus time (in seconds). Instantaneous velocities were calculated as displacement of the plus end between successive images (every 3 seconds) in a time-lapse series. The cell margin was defined as the 3-μm zone from the cell boundary. For catastrophe frequencies, the number of microtubule catastrophe events over time of observation was determined. Distribution of microtubule growing ends along the cell radius was determined by scoring the number of EB1 comets in 5 equal zones.

Western blotting, immunoprecipitation, and Rap pull-down assays

SDS-PAGE and immunoblotting with primary antibodies were done using standard protocols. Rap pull-down assays were performed as described previously.[26] For Epac1-AKAP9 coimmunoprecipitation assays, HEK 293T cells were cotransfected with Epac1-V5 and the flag-AKAP9 fragments and lysed after 48 hours in 1% NP-40, 50mM Tris-Cl (pH 8.0), 150mM NaCl buffer containing a protease inhibitor cocktail (Sigma-Aldrich). The cell lysates were precleared with protein-G Sepharose beads and incubated with protein-G Sepharose beads bound to either anti-flag or mouse immunoglobulin G (IgG). Immunoprecipitates were subjected to SDS-PAGE and immunoblotted with anti-V5 or anti-flag antibody to detect Epac1 or AKAP9, respectively.

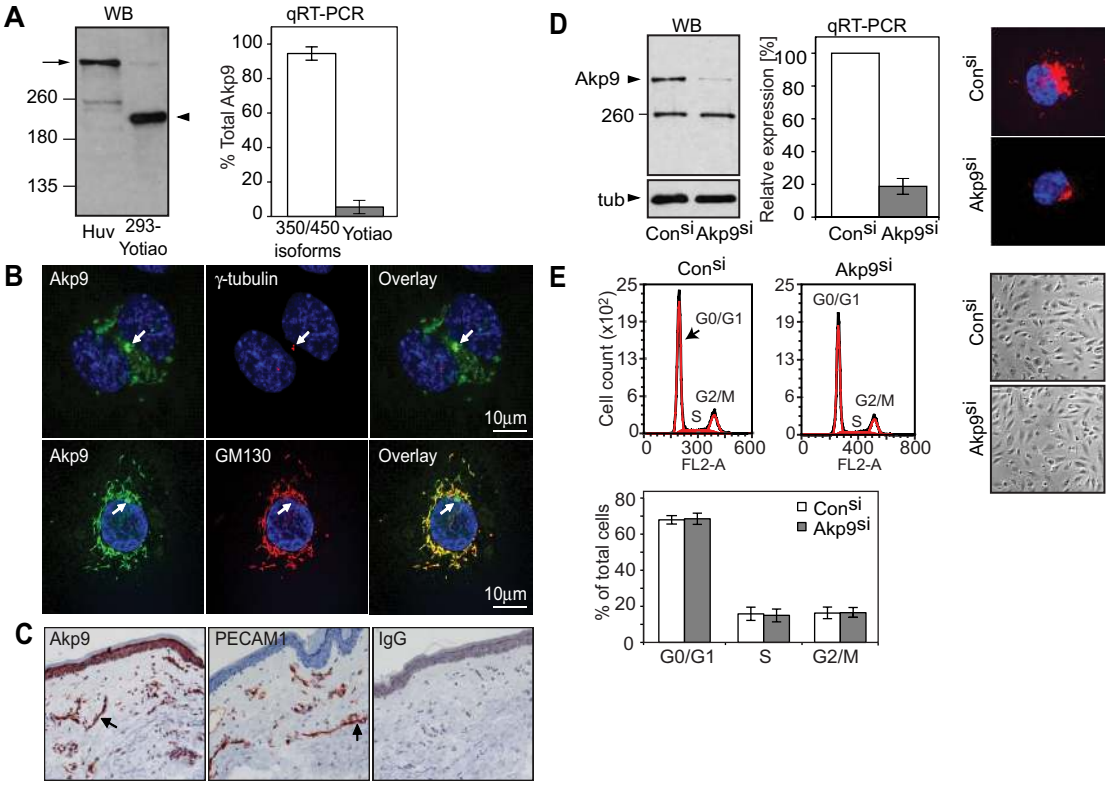

Figure 1. Analysis of AKAP9 350/450 expression in human ECs and characterization of cell cycle in AKAP9-depleted cells. (A) Left panel, Western blotting (WB) of AKAP9 in HUVEC lysate and 293 cells transfected with Yotiao (293-Yotiao). A single band at the predicted molecular weight for AKAP350/450 long isoform(s) (arrow) was observed in HUVECs. The lower 250-kD immunoreactive band in HUVECs did not migrate at the position of recombinant Yotiao in 293 cells (arrowhead). Right panel, qRT-PCR of HUVECs using primers that recognize the long isoforms (350/450 isoforms) or Yotiao was undertaken and their relative abundance (percentage of total AKAP9) was calculated. n = 4. (B) Confocal analysis of HUVECs stained with antibodies to the indicated proteins and DAPI (nucleus stain) followed by overlay of the images. AKAP9 (Akp9) codistributed with γ-tubulin, a centrosomal marker (top panel, arrow), and colocalized with GM-130, a cis-Golgi marker that is perinuclear and excludes the centrosome (bottom panel, arrow). Bar = 10 μm. (C) Tissue sections of human skin were stained with rabbit anti-Akp9, anti–PECAM-1 or rabbit IgG. AKAP9 was present in the large and small vessels (arrow) of the skin in a pattern coincident with an endothelial cell marker, PECAM-1, and in the epithelium. No specific staining was observed with IgG. (D) HUVECs were transfected with AKAP9 (Akp9) or Control (Con) siRNA duplexes (si), and evaluated 48 hours later for AKAP9 expression. Left panel, AKAP9 protein level was analyzed by Western blotting. The lower 250-kDs protein remained upon AKAP9 silencing, suggesting that it is a nonspecific, immunoreactive band. Middle panel, AKAP9 message was quantitated by qRT-PCR using oligonucleotides for long isoforms 350/450 kDa. Right panel, AKAP9 protein was assessed by immunofluorescence staining. (E) Representative cell-cycle profiles by fluorescence-activated cell sorting analysis of DNA content. Top left panel, AKAP9 silencing does not alter the distribution of cells in the different phases of the cell-cycle compared with control siRNA cells. Bottom left panel, an average of results from 3 independent experiments are given. Right panels, phase contrast images of control and AKAP9-silenced monolayers revealed an intact monolayer and cells that were morphologically similar in both cultures.

Flow cytometric analysis

HUVEC monolayers were stained for 20 minutes at 37°C with anti-integrin antibodies (β_1, α_5, and α_v) or the appropriate mouse IgG, and then rapidly trypsinized and resuspended in ice-cold PBS with 2% FCS. A donkey anti–mouse IgG Alexa-488-conjugated antibody (Invitrogen) was subsequently used and flow cytometric analysis was performed with a FACSCalibur (Becton Dickinson).

Microtubule cosedimentation assay

Microtubule cosedimentation was performed as described previously[21] with some minor modifications. Cotransfected HEK 293T cells with Epac1-flag and flag-AKAP9$^{2875\text{-}3899}$ plasmids were lysed 48 hours after transfection, in PEM buffer (100mM PIPES, pH 6.9, 1mM EGTA, 1mM $MgCl_2$) with 1% Triton X-100 containing a protease inhibitor cocktail (Sigma-Aldrich). After 30 minutes of incubation on ice to depolymerize MTs, cell lysates were centrifuged at 100 000*g* for 30 minutes at 4°C. Cleared lysates were incubated for 20 minutes at 37°C after the addition of 0.5mM GTP and 20μM taxol (Sigma-Aldrich). As negative controls, aliquots of the same cell lysates were incubated for 20 minutes on ice to prevent microtubule polymerization. Lysates were overlaid on a cushion of lysis buffer containing 20% sucrose, 0.5mM GTP and 10μM taxol, and centrifuged for 30 minutes at 30 000*g* at 25°C to sediment MTs. Microtubule pellets were washed and resuspended in Laemmli loading buffer. Samples were separated by SDS-PAGE and immunoblotted with an anti-flag antibody. The membrane was subsequently stripped and reblotted with anti-Epac1 antibody.

Measurement of endothelial transelectrical resistance and dextran leakage

Transelectrical resistance (TER) across the endothelial cell monolayer was measured using an impedance sensor system (Applied Biophysics). Data were normalized as the ratio of measured resistance to baseline resistance and plotted versus time. For integrin blocking experiments, cells were pretreated with α_v and α_5 specific antibodies or 800μM RGD or RGE for 1 hour before the addition of O-Me-cAMP.

HUVECs were plated on 0.1% gelatin-coated transwell inserts (Costar), and 48 hours later the monolayers were treated with agonists for the indicated time points. Fluorescein-dextran (500 μg/mL, 70-kDa molecular mass; Invitrogen) in Hanks balanced salt solution without phenol red was added to the top chamber, and the bottom chamber was replaced with Hanks solution 15 minutes before the end of the time point. Fluorescence in the bottom chamber was read on a microplate reader (SpectraMax M2; Molecular Devices) after 15 minutes at 37°C.

Ca^{2+} switch assay

HUVECs were cultured for 6 hours in low-Ca^{2+} medium (Eagle minimal essential medium), followed by restoration of extracellular Ca^{2+} by incubation with Eagle medium containing 1.8mM Ca^{2+}. After 1 hour, the cells were immunostained with VE-cadherin, p120, β-catenin, or dynein antibody. Images were obtained and used to calculate the intensity of immunostaining at the junctions using the line scan method from Metamorph. In this method, a line is drawn across the diameter of several cells, and the peak of fluorescence intensity, which represents the junctions, is averaged.

RGD and VE-cadherin adhesion assay

Cells were trypsinized and plated onto tissue culture plates coated with 100μM RGD or RGE peptide and incubated for 30 minutes at 37°C. The adherent cells were fixed, stained with phallodin and DAPI, and quantitated using MetaExpress software. Adhesion to RGD or RGE was also evaluated after fluorescent labeling of cells. HUVECs were labeled in suspension using 5μM CFDA labeling reagent (Vybrant; Molecular Probes), washed, incubated with 0.5% BSA-containing medium for 30 minutes at 37°C, and plated onto RGD-or RGE-coated wells. To analyze cell adhesion to VE-cadherin, 10 μg/mL VE-cadherin-Fc was immobilized on plates, and labeled cells were added in the presence or absence of O-Me-cAMP for 20 minutes at 37°C. After washing, adherent cells were quantified on a microplate reader (SpectraMax M2).

Statistical analysis

All data are presented as mean ± SD except microtubule instantaneous growth rate and length of uninterrupted growth, for which median values are given. Two-sided paired *t* test or Wilcoxon paired rank test (for median values) were performed where appropriate. $P < .05$ was considered significant.

Results

Endothelial cells express the AKAP9 long isoforms and their silencing has no effect on cell division

AKAP9 protein expression was evaluated using an antibody that detects both the long AKAP9 and the Yotiao isoforms.[27] Western blot analysis of HUVECs revealed a 400-kD AKAP9 species, while the 220-kD Yotiao was not observed (Figure 1A). Quantitative reverse transcriptase-PCR (qRT-PCR) detected mRNA for the long AKAP9 isoforms and Yotiao, but the latter represented, on average, 2% of the total AKAP9 message in HUVECs (Figure 1A). Given that the Yotiao protein was undetectable, the physiological relevance of the small pool of Yotiao message is unclear. Similar results were observed for adult HDMECs (data not shown). Thus, the long AKAP9 is the predominant isoform expressed in ECs. AKAP9 immunolocalized with GM130 (a cis-Golgi marker) and was present near the centrosomal marker γ-tubulin (Figure 1B). Immunohistochemical detection in human tissue revealed AKAP9 along with PECAM-1, an endothelial cell marker, in blood vessels and in the epidermal layer of normal human skin (Figure 1C).

To explore AKAP9 function, HUVECs were transfected with control siRNA or AKAP9 siRNA duplexes that targeted 5′-terminal sequences present in AKAP9 and Yotiao mRNA. Silencing of AKAP9 was assessed by immunoblotting and corroborated by RT-PCR and immunofluorescence (Figure 1D). Depletion of AKAP9 in HUVECs had no effect on the localization of pericentrin, another centrosomal AKAP that is structurally related to AKAP9 (supplemental Figure 1, available on the *Blood* Web site; see the Supplemental Materials link at the top of the online article).

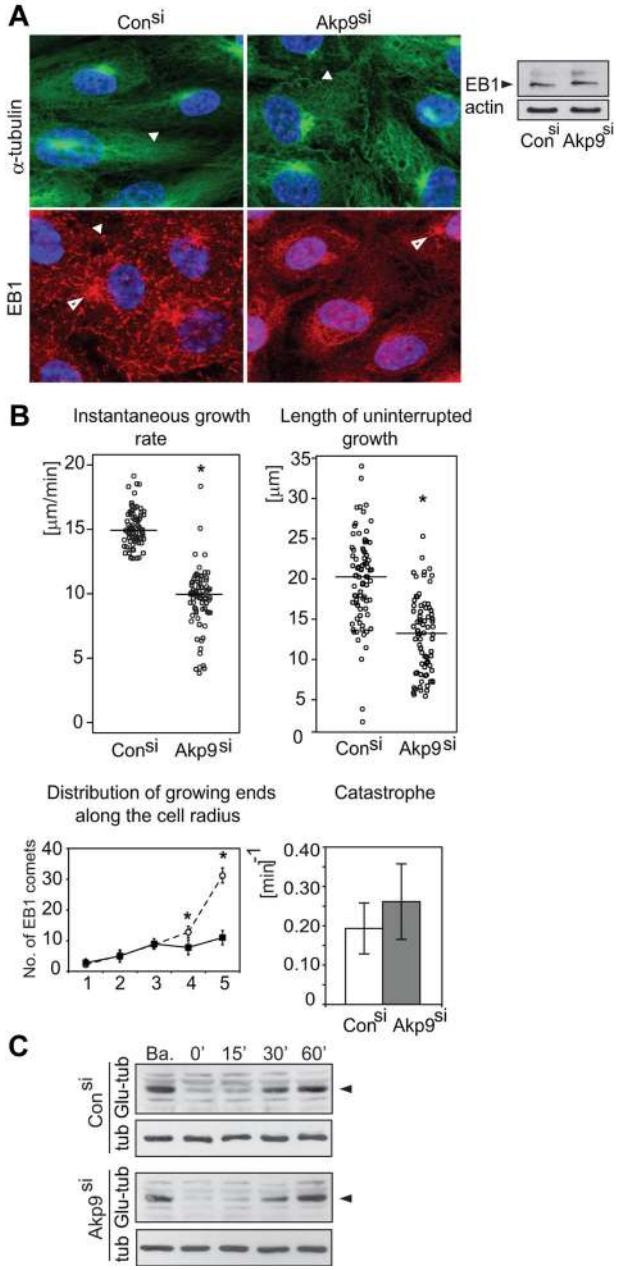

Figure 2. Defects in microtubule dynamics in AKAP9-depleted ECs. (A) HUVECs treated with control or AKAP9 siRNA were fixed and subjected to immunofluorescence microscopy using antibodies to α-tubulin or EB1. A radial network of α-tubulin positive MTs (arrowhead), EB1 as comets (arrowhead), and microtubule organizing center (MTOC, open arrowhead) were present in control siRNA-treated cells. MTs formed a disorganized network (arrowhead) in AKAP9 siRNA cells. EB1 was visible at the MTOC (open arrowhead), but appeared as dot-like structures (arrowhead) in the cytoplasm. Total EB1 levels were comparable in control and AKAP9 siRNA-treated cells, as assessed by Western blotting of cell lysates. Actin served as a loading control. (B) Live-cell analysis of GFP-EB1–transduced control and AKAP9 siRNA-treated cells. Instantaneous microtubule growth rate was calculated from the displacements of EB1-positive microtubule ends between successive frames. The length of uninterrupted growth represents the entire length of the GFP-EB1 tracks. Each data point represents the growth rate or length of a single microtubule. The horizontal bar represents the median value for 80 MTs analyzed in 10 cells per group from 3 independent experiments. Distribution of growing ends along the cell radius is calculated as the number of EB1 comets present in successive quadrants (numbered 1-5) from the centrosome to the cell periphery. Fifteen cells were analyzed. Catastrophe frequency is a measure of the number of MTs that failed to reach the cell periphery (defined as a 3-μm zone from the cell boundary) in a given time. N = 80 MTs in n = 10 cells per group collected from 3 independent experiments. *$P < .05$. (C) Lysates were prepared from control and AKAP9 siRNA cells under basal conditions (Ba) and following nocodazole treatment and subsequent washout for the indicated times in minutes. The level of Glu-tubulin was evaluated in Western blots. α-Tubulin (tub) served as a protein loading control. One of 3 representative experiments is shown.

AKAP9 depletion did not impair the ability of HUVECs to establish a confluent monolayer with the expected cobble-stone morphology, nor did it alter the DNA profiles following cell-cycle analysis (Figure 1E).

AKAP9 silencing impairs microtubule dynamics

HUVECs transfected with control or AKAP9 siRNA were immunostained for α-tubulin and plus-end-binding protein EB1. MTs organized a radial network in control siRNA-treated cells, while they formed a disordered meshwork in AKAP9-silenced cells. EB1 appeared as comet-like structures at microtubule tips in control siRNA-treated cells, as shown in other cell types.[13] In contrast, EB1 appeared as dot-like structures in AKAP9-silenced cells despite EB1 accumulation at the centrosome and overall protein levels of EB1 that were comparable to control siRNA cells (Figure 2A). This suggests that depletion of AKAP9 might alter binding of EB1 to the growing microtubule ends or that it may inhibit microtubule polymerization.

We analyzed microtubule dynamics in AKAP9-depleted confluent HUVEC monolayers by live cell imaging (Figure 2). AKAP9 depletion resulted in a significant impairment of the instantaneous growth rate, a reduction of the microtubule growth length, and accumulation of active growing ends at the cell cortex compared with control siRNA cells, whereas the microtubule catastrophe frequency was not significantly increased (Figure 2B, supplemental Videos 1-2). Consistent with the latter observation, AKAP9 depletion did not affect microtubule turnover either at steady-state or following microtubule network recovery after nocodazole washout (Figure 2C), as assessed by probing cell lysates for detyrosination of α-tubulin (Glu-tubulin). Glu-tubulin is observed after microtubule assembly, and can be used as a marker for how long a microtubule has been assembled.[28] In conclusion, AKAP9 regulates microtubule net polymerization in ECs by increasing the rate of growth while not significantly altering catastrophe events.

AKAP9 is required for Epac-induced barrier properties

We addressed the role of AKAP9 in cAMP-dependent regulation of endothelial barrier function. cAMP analogs have been extensively used to discriminate between the target proteins activated by cAMP elevation. We used a selective Epac activator, O-Me-cAMP,[29] to assess the contribution of AKAP9 in Epac-induced enhancement of barrier properties. Measurement of the TER of the monolayers allowed a time-course analysis of endothelial barrier function. AKAP9 silencing had no effect on basal permeability in a confluent monolayer of HUVECs. While O-Me-cAMP treatment increased barrier properties in control siRNA ECs, AKAP9 siRNA cells failed to enhance TER in response to Epac activation. The enhancement of TER in response to S1P, an unrelated agonist, was similar in control and AKAP9-silenced monolayers, thus establishing specificity of AKAP9's role in the cAMP/Epac-mediated pathways (Figure 3A shows cumulative data and supplemental Figure 2 shows raw data of a representative experiment). Similar TER results were obtained using a different AKAP9 siRNA sequence (data not shown). The role of AKAP9 was also confirmed in HDMECs (Figure 3B), which share with HUVECs many properties related to Epac and Rap activation.[30] Permeability to macromolecules was assessed by measuring dextran (70-kDa) flux through the endothelial monolayer. As observed with TER, baseline permeability was similar in control and

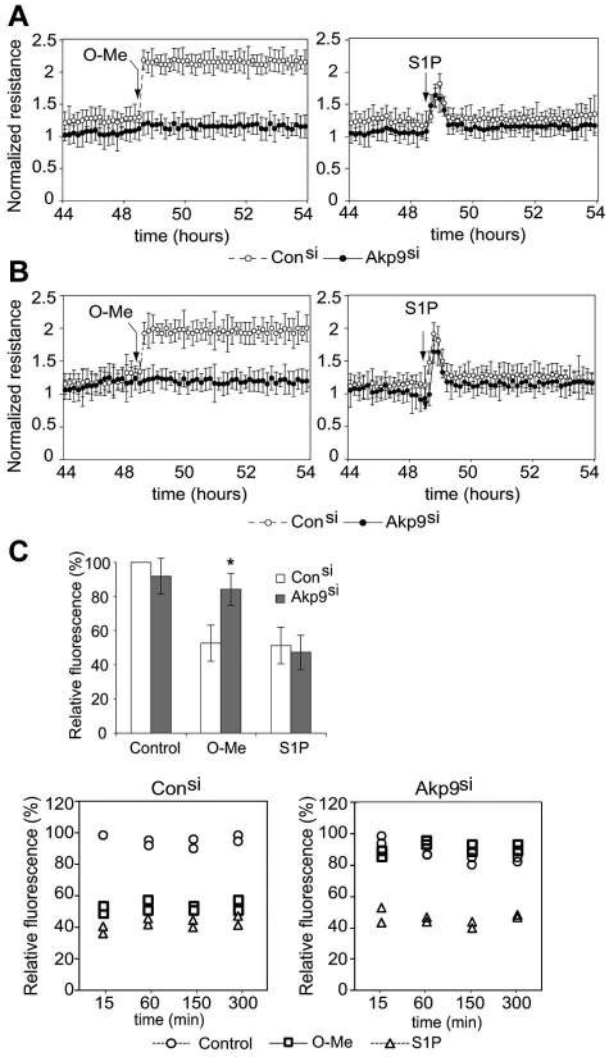

Figure 3. AKAP9-depleted cells display defects in Epac-induced enhancement of barrier properties. (A) TER of AKAP9 (Akp9^{si}) and control (Con^{si}) siRNA-treated HUVEC monolayers at baseline and following the addition of O-Me-cAMP (left panel) or S1P (right panel) at the times indicated by arrows. N = 5 experiments. (B) TER in HDMECs in response to indicated agonists. N = 3 experiments. In panels A and B, TER measurement was normalized to the resistance of the sample at time 0, which was taken 10 minutes following the addition of siRNA duplexes. Data points are average ± SD. TER data points at 45 hours and greater reflect the effects of AKAP9 silencing on resistance. AKAP9 silencing did not significantly affect basal permeability in HUVECs (A) or HDMECs (B). However, AKAP9-silenced cells fail to respond to O-Me-cAMP. (C) Top panel, dextran leakage across control siRNA and AKAP9 siRNA cell monolayers after 15 minutes of treatment with vehicle control, O-Me, or S1P (n = 3). Bottom panels, time course of dextran leakage in control (left) and AKAP9-silenced (right) cells following agonist treatment for the indicated times in minutes. One of 2 representative experiments is shown; the data represent 2 determinations (in duplicate wells) at each time point. Results are reported as a percentage of the value obtained with control siRNA at the 15-minute time point, which was set at 100%. *$P < .05$.

AKAP9 siRNA cells. O-Me-cAMP treatment prevented leakage in control siRNA HUVECs, while it failed to do so in AKAP9-depleted cells. The response to S1P was similar in control and AKAP9 siRNA cells (Figure 3C). Surprisingly, the PKA-selective cAMP analog N6-Benz-cAMP[31] similarly enhanced barrier properties in both control and AKAP9 siRNA cells (supplemental Figure 2). In summary, AKAP9 is essential for Epac-mediated increase of endothelial barrier properties, while it is dispensable for maintaining barrier properties at steady-state, and for barrier enhancement in response to PKA activation and S1P.

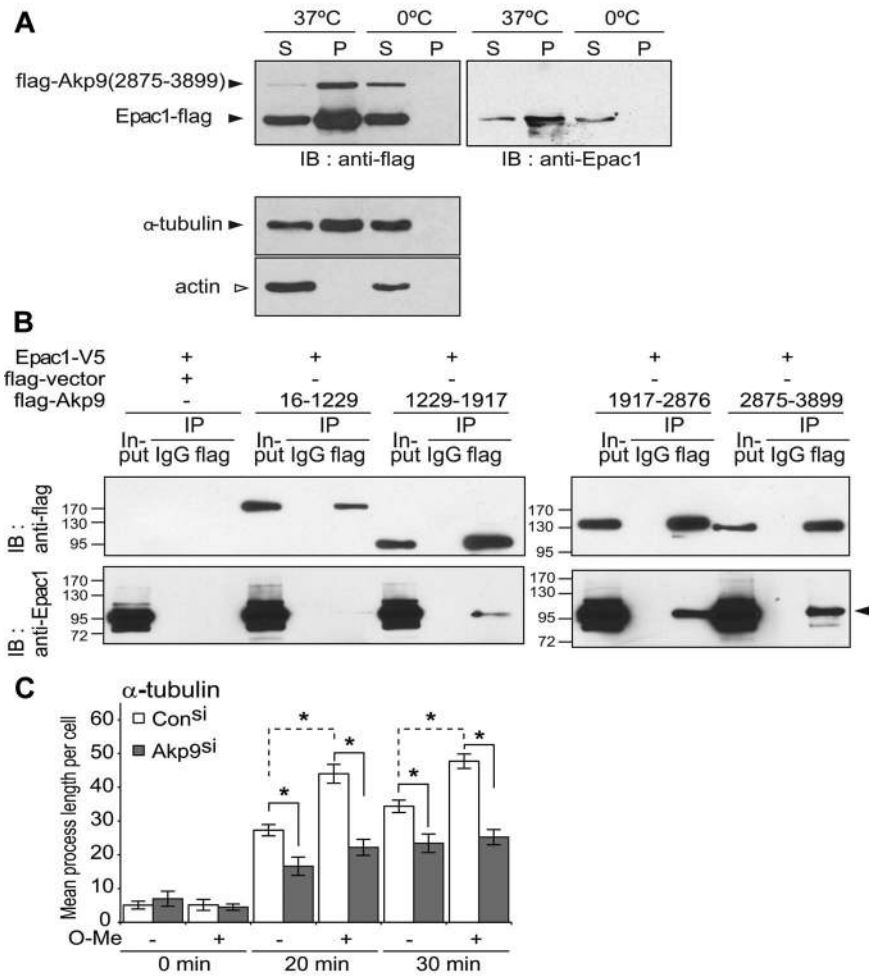

Figure 4. AKAP9 associates with Epac1 and MTs and is required for the Epac-induced increase in microtubule growth rate. (A) Cosedimentation of AKAP9 and Epac1 with MTs. Cell lysates of 293 cells transfected with flag-tagged construct of AKAP9$^{2875\text{-}3899}$ fragment and full-length Epac1 were placed on ice to depolymerize the MTs. Samples were incubated with GTP and taxol at 37°C or held on ice (0°C) (negative control). After centrifugation, the pellet sample containing polymerized MTs (P) and supernatants (S) was separated by SDS-PAGE followed by immunoblot analysis. Anti-flag antibody was used to detect Epac1 and AKAP9 (top left panel), and anti-Epac1 antibody was used to specifically identify Epac1 (right panel). Bottom panels, anti–α-tubulin versus β-actin identified the microtubule-enriched compartment (ie, tubulin positive but actin negative). Only the pellet sample at 37°C (P, 37°C) containing polymerized MTs (lacking actin) was enriched in AKAP9 and Epac1 compared with the supernatant (S, 37°C). The lower-molecular-weight anti–flag-band was confirmed to be Epac1, because it was immunoreactive with the anti-Epac1 antibody (right panel). (B) Coimmunoprecipitation of AKAP9 and Epac1. 293T cells were transfected with Epac1-V5 and flag-empty vector alone or the indicated flag-AKAP9 fragments. Lysates (Input) were immunoprecipitated (IP) with IgG control or anti-flag antibody and probed for the presence of AKAP9 and Epac by immunoblotting (IB) with anti-flag (top panel) or anti-Epac1 (bottom panel) antibodies. Epac coimmunoprecipitated only with AKAP9$^{2875\text{-}3899}$ and AKAP9$^{1917\text{-}2876}$, and weakly with AKAP9$^{1229\text{-}1917}$. For panels A and B, 1 of 3 representative experiments is shown. (C) Microtubule regrowth following nocodazole-induced depolymerization. Control (Con) and AKAP9 siRNA (Akp9)–treated HUVECs were incubated with nocodazole on ice and microtubule regrowth was quantified 20 and 30 minutes after nocodazole washout in normal (−) or O-Me-cAMP (O-Me) (+) supplemented medium at 37°C. Cells were stained for α-tubulin and the length of the MTs was determined. $^*P < .05$. n = 3 independent experiments.

AKAP9 complexes with Epac and promotes Epac-mediated net microtubule polymerization

The requirement of AKAP9 in Epac-induced endothelial barrier enhancement, together with previous reports suggesting an interaction of Epac[9,11] and AKAP9[21] with MTs, predicted that these 2 proteins may interact in a complex with MTs. Immunofluorescence staining of HUVEC monolayers failed to show AKAP9 colocalization with peripheral MTs (data not shown). This interaction, previously observed in an epithelial cell line,[21] may be transient in ECs or it may be dependent on cell-cycle or cAMP levels,[5] as is the case for Epac.[32,33] Therefore, a biochemical approach was pursued. Epac1 and a C-terminal AKAP9$^{2875\text{-}3899}$ fragment shown to have binding sites for MTs[21] were transfected into HEK 293T cells and analyzed for their ability to interact with MTs in vitro. Both Epac1 and AKAP9 cosedimented with polymerized MTs (Figure 4A), suggesting that these proteins can interact with the microtubule lattice in cells. Whether AKAP9 and Epac1 formed a complex in cells was assessed by coimmunoprecipitation approaches using Epac1 and AKAP9 fragments. Epac1 coimmunoprecipitated with AKAP9$^{2875\text{-}3899}$ and AKAP9$^{1917\text{-}3876}$, and more weakly associated with AKAP9$^{1229\text{-}1917}$ (Figure 4B). Tubulin was not observed in the coimmunoprecipitated samples (data not shown), which could reflect suboptimal conditions for maintaining polymerized MTs because these samples were processed on ice.

A net increase in microtubule length has been observed in endothelial monolayers treated with O-Me-cAMP.[11] In the present study, O-Me-cAMP was also shown to increase the net microtubule polymerization in control siRNA-treated cells during microtubule regrowth (Figure 4C), but failed to do so in AKAP9 siRNA-treated cells (Figure 4C) despite normal expression of Epac1 in these cells (supplemental Figure 3). Although O-Me-cAMP–mediated microtubule growth does not require active Rap GTPases,[11] it was, as expected, Epac dependent because silencing of Epac1 attenuated this process (supplemental Figure 3). These data suggest that Epac exerts its effect on MTs through an AKAP9-dependent pathway that does not require active Rap GTPases.

AKAP9 is not required for Epac activation of Rap GTPases, reorganization of cortical actin, or de novo VE-cadherin adhesion

To explore the mechanisms underlying the role of AKAP9 in Epac-induced barrier function, we examined whether AKAP9 was required for Epac-induced Rap activation and cortical actin and VE-cadherin homophilic interactions. After O-Me-cAMP, GTP loading of Rap GTPase in control and AKAP9 siRNA-treated cells was indistinguishable (Figure 5A). Moreover, O-Me-cAMP–induced Epac activation led to a comparable increase in cortical actin bundles and junctional VE-cadherin linearity in control and AKAP9-silenced cells (Figure 5B). Consistent with the latter observation, control and AKAP9 siRNA-treated cells similarly adhered to plate-immobilized VE-cadherin and augmented their adhesion upon stimulation with O-Me-cAMP (Figure 5C). Thus, AKAP9 is not required for the formation and maintenance of VE-cadherin homophilic interactions. To address the role of

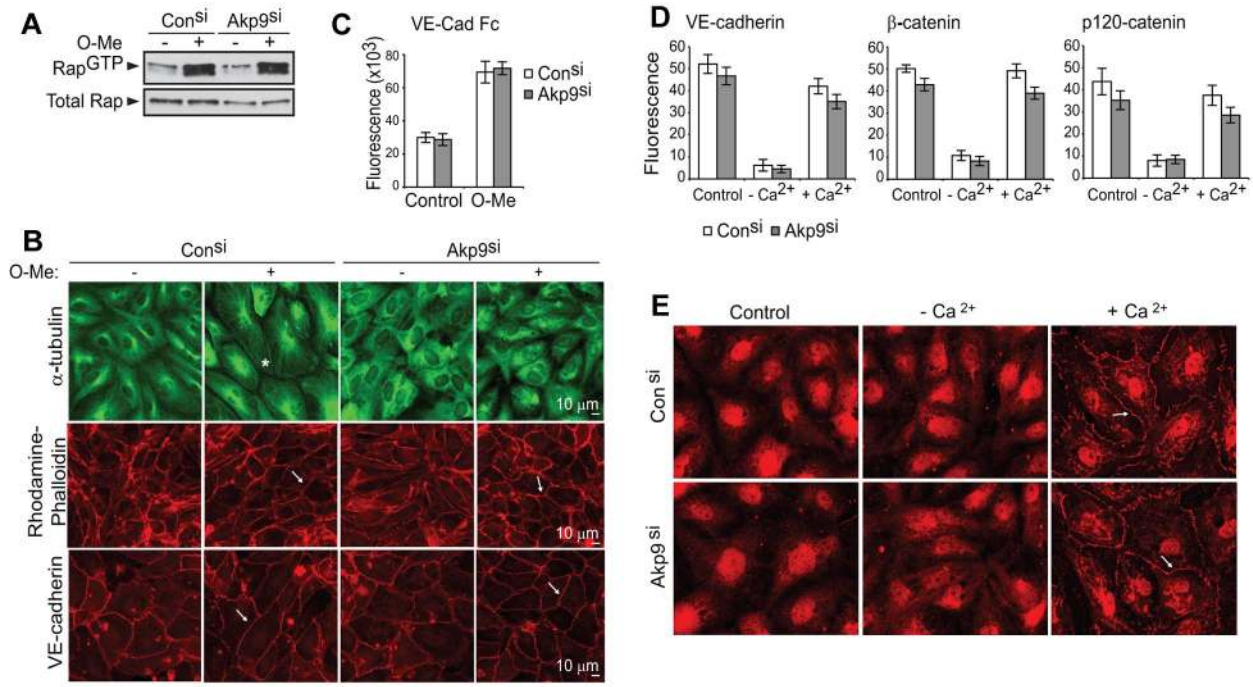

Figure 5. AKAP9 depletion does not affect Rap activation, VE-cadherin adhesion, or organization of cortical actin. Control and AKAP9 (Akp9) siRNA HUVECs were evaluated for Rap1 GTPase activity (A); microtubule distribution, actin organization, and VE-cadherin linearity at junctions (B); and VE-cadherin homophilic interactions (C), following 20 minutes of treatment with vehicle control (−) or O-Me-cAMP (+). (A) Cell lysates were subjected to pull-down assays to detect active Rap1 (Rap1GTP). O-Me-cAMP similarly enhanced Rap activation in both control and AKAP9 siRNA-treated monolayers. Western blot of total Rap1 (total Rap) shows equivalent levels of Rap1 GTPase in all samples. (B) Cells were fixed and stained for microtubule (α-tubulin), actin (rhodamine-phalloidin) or VE-cadherin. O-Me-cAMP treatment of control siRNA cells resulted in microtubule extension to the periphery of the cell (*) compared with vehicle-treated cells following O-Me-cAMP treatment, while the MTs in AKAP9-silenced cells were disorganized under either condition. In contrast, AKAP9 silencing had no effect on the ability of O-Me-cAMP to increase cortical actin bundles (arrow, middle panels) or to enhance the linearity of VE-cadherin staining (arrow, bottom panel). Scale bar = 10 μm. (C) Vybrant CFDA-labeled cells were plated on VE-cadherin Fc-coated dishes without (Control) or with O-Me-cAMP (O-Me) treatment, and cell adhesion was quantified by fluorometric analysis. (D) Analysis of de novo AJ formation. Cells were cultured in complete medium (Control), placed in low-Ca^{2+} medium ($-Ca^{2+}$), and then in medium replenished with Ca^{2+} ($+Ca^{2+}$). Cell samples were fixed at these different phases and immunostained for VE-cadherin, β-catenin, or p120 as indicated, and fluorescence intensity at junctions was determined. (E) Analysis of dynein distribution. Control and AKAP9 siRNA cells were subjected to the Ca^{2+} switch assay, as described in panel D, and stained for dynein. Dynein was initially absent at the junctions of cells, but similarly appeared at cell-cell contacts (arrow) of control and AKAP9 siRNA cells following Ca^{2+} replenishment ($+Ca^{2+}$). n = 3 for experiments in panels A through E.

AKAP9 in de novo assembly of VE-cadherin adhesion at AJs, we pursued a Ca^{2+} switch strategy. ECs cultured in the presence of EGTA lose Ca^{2+}-dependent, homotypic interactions of junctional VE-cadherin and associated proteins, while subsequent Ca^{2+} replenishment reverses this process.[34] Ca^{2+} depletion induced disassembly of VE-cadherin adhesion and Ca^{2+} repletion led to reappearance of VE-cadherin and its associated catenins at cell-cell contacts in both control and AKAP9-silenced monolayers (Figure 5D). In addition to catenins, the minus-end-directed microtubule motor protein dynein, which is known to associate with a AKAP9-binding partner, dynactin,[21] interacts with β-catenin at the AJs of epithelial cells to capture microtubule plus ends and to facilitate the formation of nascent junctions.[35] Dynein was not observed at cell-cell contacts of resting, confluent ECs, but was rapidly and transiently localized to AJs following Ca^{2+} switch in both control and AKAP9 siRNA cells (Figure 5E).

In summary, AKAP9 is not essential for relaying Epac effects on Rap GTPase activation and the accompanying changes in the organization of cortical actin, or for VE-cadherin homophilic adhesion and localization of VE-cadherin and associated catenins and dynactin at junctions.

AKAP9-mediated adhesion of integrins contributes to Epac-induced enhancement of barrier properties

Given the absence of changes in VE-cadherin homophilic interactions in AKAP9-silenced cells, we explored the possibility that AKAP9 promotes Epac-induced barrier properties by supporting integrin-mediated adhesion. AKAP9 silencing led to a significant defect in the ability of suspended cells to adhere to immobilized RGD peptide compared with control siRNA cells (Figure 6A), despite similar integrin cell surface expression in both groups (Figure 6B). Although O-Me-cAMP was shown to increase integrin adhesion to RGD in an ovarian carcinoma cell line,[36] it did not enhance endothelial cell adhesion to RGD (data not shown). Epac1 silencing did reduce their ability to bind RGD (Figure 6A), indicating that endogenous Epac1 activity promotes integrin-mediated adhesion. Interestingly, Epac siRNA resulted in a significant change in the organization of actin in the cells that did adhere to RGD compared with adherent control siRNA and AKAP9 siRNA cells (Figure 6A). These data support the model that, while the Epac/AKAP9 axis is not essential for cortical actin reorganization, Epac activation of Rap likely drives this process.

The contribution of RGD integrins specifically to the Epac-induced increase in barrier properties was evaluated. Prolonged treatment with soluble RGD peptide increased permeability in HUVECs plated on either fibronectin or collagen type IV. Pretreatment with RGD peptide for 1 hour had no effect on baseline permeability but significantly impaired O-Me-cAMP–induced enhancement of barrier function on both matrices (Figure 6C). To identify the RGD integrins involved, we evaluated the effect of functional blocking antibodies to α_5 and α_v, previously identified at cell-cell contacts,[4] on barrier function. Unexpectedly, functional

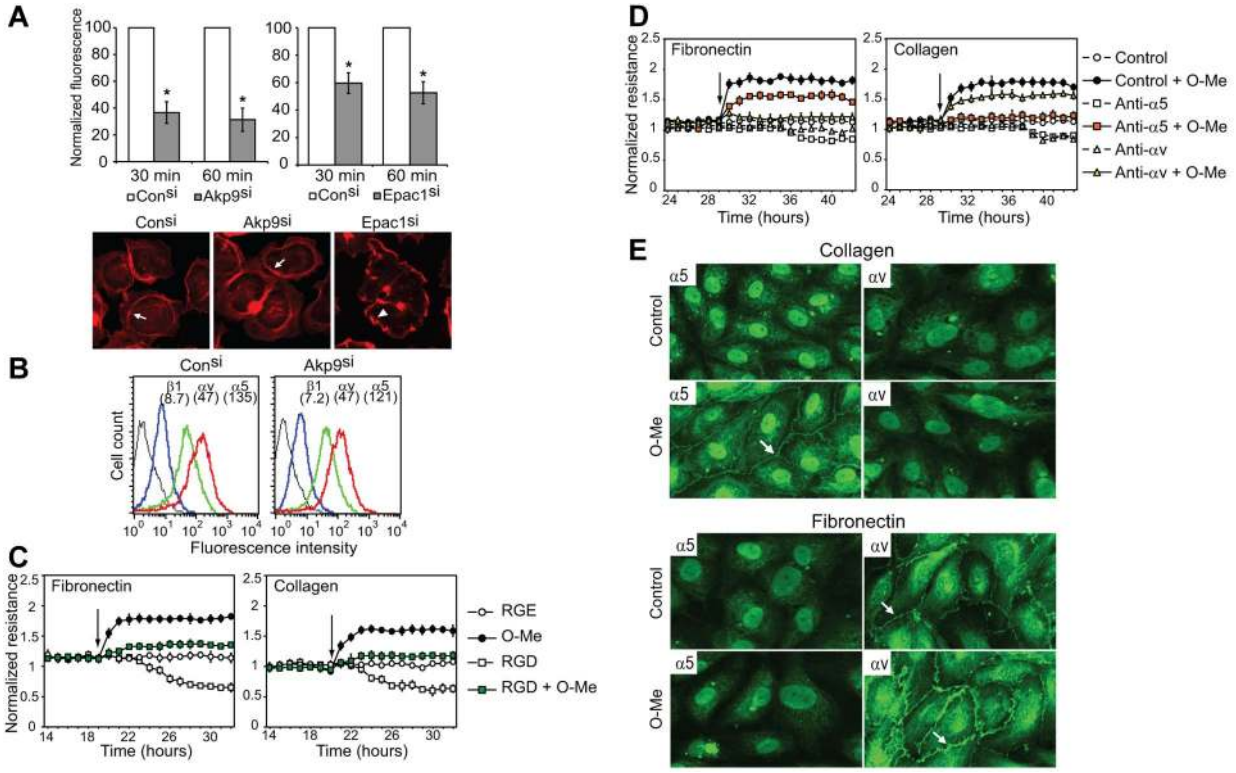

Figure 6. AKAP9 is required for integrin-mediated adhesion, and Epac increases barrier properties through RGD-binding integrins at lateral cell borders. (A) Fluorescently labeled control siRNA, AKAP9 siRNA, or Epac1siRNA transfected cells were incubated on RGD-coated plates and cell adhesion was quantified by fluorometric analysis. Data, averaged from 3 experiments, are plotted relative to control siRNA (set at 100%). $P < .005$. Cells were stained with rhodamine-phalloidin to visualize actin. Actin was present in a cortical ring (arrow, Con^{si} and AKAP^{si}) or membrane edge (arrowhead, Epac^{si}). (B) Control and AKAP9 siRNA-treated cells were stained with antibody to β_1 (blue), α_v (green), or α_5 (red) and analyzed by flow cytometry; mean fluorescence intensities for each are in brackets. Data using isotype IgG are shown in black. One of 2 representative experiments is shown. (C-D) HUVECs were plated on fibronectin or collagen type IV. TER was evaluated in HUVECs treated with RGD or control (RGE) peptides (C) or functional blocking integrin antibodies (D) 1 hour before the addition of vehicle control or O-Me-cAMP (O-Me) at the time points indicated by the arrows. RGD treatment decreased basal permeability over time and reduced O-Me-cAMP-induced enhancement of barrier properties compared with RGE peptide treatment. α_v antibody attenuated O-Me-cAMP-induced effects on cells plated on fibronectin, while α_5 antibody blocked O-Me-cAMP effects on collagen. n = 3-5 experiments. (E) ECs plated on collagen (top panels) or fibronectin (bottom panels) were stimulated with vehicle control (Control) or O-Me-cAMP (O-Me) and stained with antibody to α_5 or α_v. α_5 and α_v were absent at lateral borders of cells plated on collagen, but α_5 appeared at cell-cell contacts (arrow) following O-Me-cAMP treatment. α_v was present at cell-cell contacts of cells plated on fibronectin (arrow) and increased there after O-Me-cAMP treatment (arrow), while α_5 remained absent even after O-Me-cAMP stimulation. One of 2 representative experiments is shown.

blocking antibody to α_v only effectively inhibited O-Me-cAMP effects on cells plated on fibronectin, while α_5 antibody had a marked effect only on cells cultured on collagen (Figure 6D). The differential effects of the blocking antibodies prompted us to examine the distribution of integrins on cells adherent to fibronectin and collagen. α_v immunolocalized to cell-cell contacts of cells plated on fibronectin, but not collagen, and its levels increased following O-Me-cAMP treatment (Figure 6E). α_5 was absent at the borders of cells adherent to either collagen or fibronectin, but upon O-Me-cAMP treatment, appeared only at junctions of cells plated on collagen (Figure 6E). Thus, O-Me-cAMP increases the accumulation of α_v at cell-cell contacts of cells adherent to fibronectin and redistributes α_5 to junctions in cells plated on collagen. The correlation between a particular integrin at the junctions and its role in O-Me-cAMP–induced barrier function infers that integrins at cell-cell contacts play primary roles in enhancing barrier properties following Epac activation. We were unable to determine the effect of AKAP9 silencing on integrin redistribution following O-Me-cAMP treatment, because the electroporation technique to introduce siRNA resulted in the loss of detectability of integrins at lateral borders. However, we propose that integrins did contribute to barrier function even under these conditions, because RGD inhibited barrier enhancement by O-Me-cAMP in control siRNA cells (data not shown).

Discussion

Our results describe a role for AKAP9 in regulating microtubule dynamics and enhancing endothelial barrier downstream of Epac activation. Whereas AKAP9 is required for persistent microtubule growth under steady-state conditions, it was found not to be essential for maintaining basal barrier properties. Instead, it was required when the cell was challenged to make new adhesive contacts, as is the case when Epac activation promotes adhesion at cell-cell contacts to enhance barrier function. Collectively, these findings are important for several reasons. First, they uncover new biological roles for AKAP9 that appear distinct from those of Yotiao, the well-described shorter AKAP9 isoform. Yotiao, present at the plasma membrane, interacts with the N-methyl D-aspartate receptor to modulate its activity at synapses and with a cardiac potassium channel to regulate the repolarization of the heart.[14,27] Second, because AKAP9 silencing affected microtubule growth, it allowed us to link microtubule dynamics to specific endothelial cell responses. Third, the data provide compelling genetic

evidence for a new pathway by which Epac relays cAMP signals to effector functions independently of its exchange factor activity toward Rap GTPases. Fourth, the work reveals a primary role for integrin-mediated adhesive interactions at cell-cell contacts in regulating Epac1/AKAP9-mediated barrier properties. The role of AKAP9 may be attributed to its observed localization in the Golgi and/or the centrosomal compartment in ECs under basal conditions, known microtubule nucleation sites. The subcellular distribution of AKAP9 may be dynamic, because it has been described on MTs during their regrowth[21] and also at cell-cell borders.[37] AKAP9 formed a ternary complex with MTs and Epac1 in vitro, suggesting its potential to interact with growing MTs in vivo. Further clarification of the conditions under which AKAP9 and Epac1 bind MTs in vivo is required to determine whether AKAP9 regulates microtubule remodeling locally or from microtubule organizing centers. Immunohistochemical detection in human tissue revealed AKAP9 primarily in blood vessels and in the epidermal layer of normal skin. The relative abundance of AKAP9 in cells with well-developed junctions, such as the endothelium and epithelium, may predict tissue-specific roles for AKAP9 in vivo.

In several cell types, MTs can be nucleated at centrosomal and noncentrosomal sites. Recent studies indicate that AKAP9 is required for microtubule nucleation at the cis-Golgi following recovery from microtubule depolymerization.[16] AKAP9 may also be required for the anchoring and release of MTs from the centrosome, although both AKAP9 and kendrin/pericentrin-B are required for nucleation from isolated centrosomal preparations,[38] indicating that AKAP9 alone is not sufficient for this process. The reduction in EB1 concentration at the microtubule tips of AKAP9-depleted ECs suggested changes in the growth properties of MTs, because EB1 is associated with growing, but not pausing or depolymerizing, microtubule ends.[39] Furthermore, conclusive roles for AKAP9 in the microtubule polymerization rate, a specific aspect of microtubule dynamics, was obtained by live-cell imaging. Despite the change in microtubule growth in AKAP9-silenced cells, the stability of MTs, which is promoted by their capture at the cell cortex,[40] was unaffected. In epithelial cells, dynein (a minus-end-directed microtubule motor protein) associates with β-catenin at AJs and binds microtubule +TIPs to facilitate the delivery of junctional components,[12] and its localization requires an intact actin cytoskeleton.[41] Dynein also interacts with AKAP9.[21] We show that dynein transiently appeared at newly forming junctions of ECs, and that this was not dependent on AKAP9. AKAP9 was also not required for the localization of VE-cadherin, p120, and β-catenin at nascent junctions, nor was it essential for VE-cadherin homophilic adhesion. These data support the conclusion that cortical actin and receptor complexes potentially required for microtubule capture at junctions distribute normally in the relative absence of AKAP9. It remains possible that perturbation of microtubule dynamics in AKAP9-silenced cells has consequences for other junctional processes affecting endothelial barrier properties that were not directly measured in our study.

The contribution of AKAP9 in the Epac-mediated increase in barrier properties and microtubule regrowth was striking. Our biochemical coimmunoprecipitation approach suggests that, like PKA, Epac can potentially interact with AKAP9 through multiple sites. The interaction(s) could be direct or facilitated via intermediate binding partners such as protein phosphatase 2A and PDE4D3, both of which bind both AKAP9[42,43] and Epac[6,44] and both of which have binding sites in the AKAP9 fragments that coimmunoprecipitate Epac1. The possibility also exists that AKAP9-mediated microtubule growth delivers active Epac to specific locations,

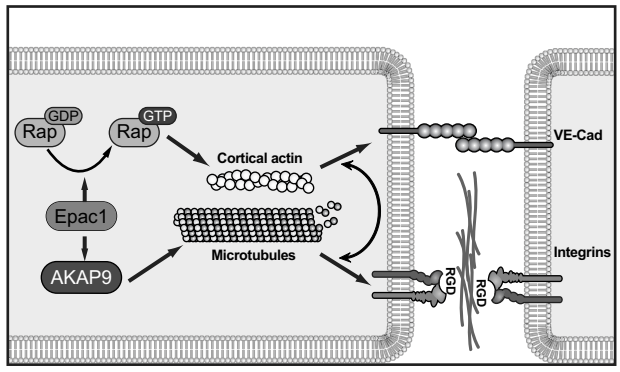

Figure 7. Model of cAMP/Epac1-induced endothelial barrier function requiring integrins. cAMP activation of Epac1 triggers 2 pathways: Epac mediates GTP-loading of Rap GTPases, which promotes cortical actin and VE-cadherin-induced cell-cell adhesion, and Epac activation of AKAP9 promotes microtubule growth. This pathway drives integrin adhesion at cell-cell borders. The coordinated function of VE-cadherin and integrins at junctional sites enhances endothelial cell barrier properties in response to cAMP-mediated activation of Epac.

which does not a priori require AKAP9 and Epac1 to be in a complex. Under conditions of AKAP9 depletion that resulted in defects in Epac-induced enhancement of barrier properties, there was a surprising lack of effect on Epac-induced Rap activation. Because it is well-accepted that Rap is required for Epac-induced enhancement of barrier function, we propose that Epac in complex with AKAP9 promotes microtubule growth, thus creating tracks for delivery of Rap effectors to AJs, where Rap is localized.[26,45] Thus, although Rap activation per se does not require AKAP9, the effectors of Rap likely require AKAP9 to promote junction strengthening (Figure 7).

The lack of effect of AKAP9 silencing on Epac-induced VE-cadherin homophilic adhesion and localization left unanswered the question of how the Epac/AKAP9 axis regulates barrier properties. In a stable, mature endothelial monolayer, functional blockade of paxillin or the RGD-binding integrins increases vascular permeability,[3,4,46] and RGD peptides induce vascular permeability in vivo.[3] AKAP9 was required for de novo integrin-mediated adhesion. Epac1 silencing also resulted in a reduction in integrin-mediated adhesion, but it remains a possibility that AKAP9 affects additional integrin-dependent functions that are independent of Epac activity. The requirement for RGD-binding integrin α_v versus α_5 in O-Me-cAMP-induced barrier properties was coincident with the presence of that integrin at cell-cell contacts, thus supporting the argument that the junctional pool of integrins contributes to barrier enhancement. The mechanism for differential integrin localization that is dependent on the substratum is not clear, but we reason that on fibronectin, α_5, the principal fibronectin-binding integrin, is sequestered primarily at cell-matrix sites, while α_v, which has a much lower affinity for fibronectin than $\alpha_5\beta_1$,[47] preferentially localizes to the cell-cell border. Conversely, on collagen, α_v binds collagen[48] at the abluminal surface and α_5 is enriched at the cell-cell interface. The ligand(s) at the cell-cell border for RGD-binding integrins are likely extracellular matrix proteins such as fibronectin, laminin, and collagen type IV, which are produced by the endothelium and concentrated at lateral cell-cell contacts.[4] Previous work suggests that vascular endothelial growth factor (VEGF)–induced permeability is also dependent on integrins,[49] whereas in our case, integrins increased barrier function. One possible explanation for this is that VE-cadherin recycling in resting monolayers is regulated by integrins and that this parameter is differentially influenced by VEGF and Epac.

VE-cadherin and integrins likely play codominant roles in junctional remodeling, because their functions are not mutually exclusive.[50] We propose that Epac activation of Rap at junctions enhances cortical actin, which drives VE-cadherin homophilic interactions and assembly of cortical complexes. The assembled complexes capture MTs, the persistent growth of which is dependent on Epac/AKAP9 activity. These MTs may deliver factors such as the Rap effectors RapL and KRIT-1, which bind MTs[51-53] and regulate integrins[54] to promote integrin function at AJs (Figure 7).

In conclusion, AKAP9 is a central player in microtubule dynamics in human ECs that is linked to the ability of the endothelial monolayer to regulate its barrier properties in response to cAMP-mediated Epac1 activation. AKAP9 is required for integrin-mediated adhesion, and this property at cell-cell contacts contributes to the Epac1-induced enhancement of barrier function. Our studies suggest that AKAP9 may be important in relaying other Epac-regulated cellular responses, from insulin secretion and neurotransmitter release to leukocyte activation and cardiac contraction.[8] Identifying the contribution of AKAP9, a member of the AKAP family of proteins that are known to temporally and spatially compartmentalize cAMP-induced signals, to specific Epac functions may help to explain how Epac fulfills its diverse roles within a single cell.

Acknowledgments

We thank George Stavrakis in the Morphology Support Core facility for immunostaining of tissue. We are grateful to Drs Lei Chen and Robert Kass (Columbia University, New York, NY) for anti-AKAP9 antibody, to Dr Kerry S. Campbell (Fox Chase Cancer Center, Philadelphia, PA) for anti-dynein light chain antibody, and to Dr G. G. Gunderson (Columbia University) for antibody against Glu-tubulin. We thank Dr Andrew P. Kowalczyk (Emory University, Atlanta, GA) for the kind gift of HDMEC. We thank Drs Francis W. Luscinskas and Andrew Lichtman for valuable discussions.

This work was supported by the National Institutes of Health, PO1HL036028 and RO1 DK51643 (to T.M.), KO1 AR054984 (to X.C.) and by a scholarship from the Norvartis Foundation (formerly Ciba-Geigy-Jubilee Foundation; to T.E.).

Authorship

Contribution: S.S., T.E., and X.C. designed and performed the research, analyzed the data, and made the figures; Y.K. aided in the analysis and interpretation of the data; M.T. and Y.O. provided valuable reagents; T.N.M. designed the research, analyzed the data, and wrote the paper; and S.S., T.E., X.C., and Y.K. revised the paper for important intellectual content.

Conflict-of-interest disclosure: The authors declare no competing financial interests.

Correspondence: Tanya N. Mayadas, Professor of Pathology, Brigham and Women's Hospital and Harvard Medical School, 77 Avenue Louis Pasteur NRB 752O, Boston, MA 02115; e-mail: tmayadas@rics.bwh.harvard.edu.

References

1. Vestweber D. VE-cadherin: the major endothelial adhesion molecule controlling cellular junctions and blood vessel formation. *Arterioscler Thromb Vasc Biol.* 2008;28(2):223-232.
2. Mehta D, Malik AB. Signaling mechanisms regulating endothelial permeability. *Physiol Rev.* 2006; 86(1):279-367.
3. Wu MH, Ustinova E, Granger HJ. Integrin binding to fibronectin and vitronectin maintains the barrier function of isolated porcine coronary venules. *J Physiol.* 2001;532(Pt 3):785-791.
4. Lampugnani MG, Resnati M, Dejana E, Marchisio PC. The role of integrins in the maintenance of endothelial monolayer integrity. *J Cell Biol.* 1991;112(3):479-490.
5. Taskén K, Aandahl EM. Localized effects of cAMP mediated by distinct routes of protein kinase A. *Physiol Rev.* 2004;84:137-167.
6. Dodge-Kafka KL, Soughayer J, Pare GC, et al. The protein kinase A anchoring protein mAKAP coordinates two integrated cAMP effector pathways. *Nature.* 2005;437:574-578.
7. Nijholt IM, Dolga AM, Ostroveanu A, Luiten PG, Schmidt M, Eisel UL. Neuronal AKAP150 coordinates PKA and Epac-mediated PKB/Akt phosphorylation. *Cell Signal.* 2008;20(10):1715-1724.
8. Gloerich M, Bos JL. Epac: defining a new mechanism for cAMP action. *Annu Rev Pharmacol Toxicol.* 2010;50:355-375.
9. Yarwood SJ. Microtubule-associated proteins (MAPs) regulate cAMP signalling through exchange protein directly activated by cAMP (EPAC). *Biochem Soc Trans.* 2005;33(6):1327-1329.
10. Mei FC, Cheng X. Interplay between exchange protein directly activated by cAMP (Epac) and microtubule cytoskeleton. *Mol Biosyst.* 2005;1: 325-331.
11. Sehrawat S, Cullere X, Patel S, Italiano J Jr, Mayadas TN. Role of Epac1, an exchange factor for Rap GTPases, in endothelial microtubule dynamics and barrier function. *Mol Biol Cell.* 2008; 19(3):1261-1270.
12. Stehbens SJ, Akhmanova A, Yap AS. Microtubules and cadherins: a neglected partnership. *Front Biosci.* 2009;14:3159-3167.
13. Akhmanova A, Steinmetz MO. Tracking the ends: a dynamic protein network controls the fate of microtubule tips. *Nat Rev Mol Cell Biol.* 2008;9(4):309-322.
14. Wong W, Scott JD. AKAP signalling complexes: Focal points in space and time. *Nat Rev Mol Cell Biol.* 2004;5(12):959-970.
15. Larocca MC, Jin M, Goldenring JR. AKAP350 modulates microtubule dynamics. *Eur J Cell Biol.* 2006;85(7):611-619.
16. Rivero S, Cardenas J, Bornens M, Rios RM. Microtubule nucleation at the cis-side of the Golgi apparatus requires AKAP450 and GM130. *EMBO J.* 2009;28(8):1016-1028.
17. Chen L, Kurokawa J, Kass RS. Phosphorylation of the A-kinase-anchoring protein Yotiao contributes to protein kinase A regulation of a heart potassium channel. *J Biol Chem.* 2005;280(36): 31347-31352.
18. Campbell KS, Cooper S, Dessing M, Yates S, Buder A. Interaction of p59fyn kinase with the dynein light chain, Tctex-1, and colocalization during cytokinesis. *J Immunol.* 1998;161(4):1728-1737.
19. Gundersen GG, Kalnoski MH, Bulinski JC. Distinct populations of microtubules: tyrosinated and nontyrosinated alpha tubulin are distributed differently in vivo. *Cell.* 1984;38(3):779-789.
20. Stepanova T, Slemmer J, Hoogenraad CC, et al. Visualization of microtubule growth in cultured neurons via the use of EB3-GFP (end-binding protein 3-green fluorescent protein). *J Neurosci.* 2003;23(7):2655-2664.
21. Kim HS, Takahashi M, Matsuo K, Ono Y. Recruitment of CG-NAP to the Golgi apparatus through interaction with dynein-dynactin complex. *Genes Cells.* 2007;12(3):421-434.
22. Mei FC, Qiao J, Tsygankova OM, Meinkoth JL, Quilliam LA, Cheng X. Differential signaling of cyclic AMP: opposing effects of exchange protein directly activated by cyclic AMP and cAMP-dependent protein kinase on protein kinase B activation. *J Biol Chem.* 2002;277(13):11497-11504.
23. Livak KJ, Schmittgen TD. Analysis of relative gene expression data using real-time quantitative PCR and the 2(-Delta Delta C(T)) Method. *Methods.* 2001;25(4):402-408.
24. Tudor EL, Perkinton MS, Schmidt A, et al. ALS2/Alsin regulates. Rac-PAK signaling and neurite outgrowth. *J Biol Chem.* 2005;280(41):34735-34740.
25. Komarova YA, Vorobjev IA, Borisy GG. Life cycle of MTs: persistent growth in the cell interior, asymmetric transition frequencies and effects of the cell boundary. *J Cell Sci.* 2002;115(Pt 17): 3527-3539.
26. Cullere X, Shaw SK, Andersson L, Hirahashi J, Luscinskas FW, Mayadas TN. Regulation of vascular endothelial barrier function by Epac, a cAMP-activated exchange factor for Rap GTPase. *Blood.* 2005;105(5):1950-1955.
27. Chen L, Marquardt ML, Tester DJ, Sampson KJ, Ackerman MJ, Kass RS. Mutation of an A-kinase-anchoring protein causes long-QT syndrome. *Proc Natl Acad Sci U S A.* 2007;104(52):20990-20995.
28. Westermann S, Weber K. Post-translational modifications regulate microtubule function. *Nat Rev Mol Cell Biol.* 2003;4(12):938-947.
29. Bos JL. Epac proteins: multi-purpose cAMP targets. *Trends Biochem Sci.* 2006;31(12):680-686.
30. Baumer Y, Drenckhahn D, Waschke J. cAMP induced Rac 1-mediated cytoskeletal reorganization

in microvascular endothelium. *Histochem Cell Biol.* 2008;129(6):765-778.

31. Poppe H, Rybalkin SD, Rehmann H, et al. Cyclic nucleotide analogs as probes of signaling pathways. *Nat Methods.* 2008;5(4):277-278.
32. Qiao J, Mei FC, Popov VL, Vergara LA, Cheng X. Cell cycle-dependent subcellular localization of exchange factor directly activated by cAMP. *J Biol Chem.* 2002;277(29):26581-26586.
33. Magiera MM, Gupta M, Rundell CJ, Satish N, Ernens I, Yarwood SJ. Exchange protein directly activated by cAMP (EPAC) interacts with the light chain (LC) 2 of MAP1A. *Biochem J.* 2004;382(Pt 3):803-810.
34. Lampugnani MG, Corada M, Caveda L, et al. The molecular organization of endothelial cell to cell junctions: differential association of plakoglobin, beta-catenin, and alpha-catenin with vascular endothelial cadherin (VE-cadherin). *J Cell Biol.* 1995;129(1):203-217.
35. Ligon LA, Holzbaur EL. Microtubules tethered at epithelial cell junctions by dynein facilitate efficient junction assembly. *Traffic.* 2007;8(7):808-819.
36. Rangarajan S, Enserink JM, Kuiperij HB, et al. Cyclic AMP induces integrin-mediated cell adhesion through Epac and Rap1 upon stimulation of the beta 2-adrenergic receptor. *J Cell Biol.* 2003; 160(4):487-493.
37. Berryman MA, Goldenring JR. CLIC4 is enriched at cell-cell junctions and colocalizes with AKAP350 at the centrosome and midbody of cultured mammalian cells. *Cell Motil Cytoskeleton.* 2003;56(3):159-172.
38. Takahashi M, Yamagiwa A, Nishimura T, Mukai H, Ono Y. Centrosomal proteins CG-NAP and kendrin provide microtubule nucleation sites by anchoring gamma-tubulin ring complex. *Mol Biol Cell.* 2002;13(9):3235-3245.
39. Morrison EE, Wardleworth BN, Askham JM, Markham AF, Meredith DM. EB1, a protein which interacts with the APC tumour suppressor, is associated with the microtubule cytoskeleton throughout the cell cycle. *Oncogene.* 1998; 17(26):3471-3477.
40. Gundersen GG, Gomes ER, Wen Y. Cortical control of microtubule stability and polarization. *Curr Opin Cell Biol.* 2004;16(1):106-112.
41. Ligon LA, Karki S, Tokito M, Holzbaur EL. Dynein binds to beta-catenin and may tether microtubules at adherens junctions. *Nat Cell Biol.* 2001; 3(10):913-917.
42. Taskén KA, Collas P, Kemmner WA, Witczak O, Conti M, Tasken K. Phosphodiesterase 4D and protein kinase a type II constitute a signaling unit in the centrosomal area. *J Biol Chem.* 2001; 276(25):21999-22002.
43. Takahashi M, Shibata H, Shimakawa M, Miyamoto M, Mukai H, Ono Y. Characterization of a novel giant scaffolding protein, CG-NAP, that anchors multiple signaling enzymes to centrosome and the golgi apparatus. *J Biol Chem.* 1999;274(24):17267-17274.
44. Hong K, Lou L, Gupta S, Ribeiro-Neto F, Altschuler DL. A novel Epac-Rap-PP2A signaling module controls cAMP-dependent Akt regulation. *J Biol Chem.* 2008;283(34):23129-23138.
45. Sakurai A, Fukuhara S, Yamagishi A, et al. MAGI-1 is required for Rap1 activation upon cell-cell contact and for enhancement of vascular endothelial cadherin-mediated cell adhesion. *Mol Biol Cell.* 2006;17(2):966-976.
46. Birukova AA, Cokic I, Moldobaeva N, Birukov KG. Paxillin is involved in the differential regulation of endothelial barrier by HGF and VEGF. *Am J Respir Cell Mol Biol.* 2009;40(1):99-107.
47. Zhang Z, Morla AO, Vuori K, Bauer JS, Juliano RL, Ruoslahti E. The alpha v beta 1 integrin functions as a fibronectin receptor but does not support fibronectin matrix assembly and cell migration on fibronectin. *J Cell Biol.* 1993;122(1):235-242.
48. Pedchenko V, Zent R, Hudson BG. Alpha(v)beta3 and alpha(v)beta5 integrins bind both the proximal RGD site and non-RGD motifs within noncollagenous (NC1) domain of the alpha3 chain of type IV collagen: implication for the mechanism of endothelia cell adhesion. *J Biol Chem.* 2004; 279(4):2772-2780.
49. Su G, Hodnett M, Wu N, et al. Integrin alphav-beta5 regulates lung vascular permeability and pulmonary endothelial barrier function. *Am J Respir Cell Mol Biol.* 2007;36(3):377-386.
50. Chen X, Gumbiner BM. Crosstalk between different adhesion molecules. *Curr Opin Cell Biol.* 2006;18(5):572-578.
51. Glading A, Han J, Stockton RA, Ginsberg MH. KRIT-1/CCM1 is a Rap1 effector that regulates endothelial cell cell junctions. *J Cell Biol.* 2007; 179(2):247-254.
52. Fujita H, Fukuhara S, Sakurai A, et al. Local activation of Rap1 contributes to directional vascular endothelial cell migration accompanied by extension of microtubules on which RAPL, a Rap1-associating molecule, localizes. *J Biol Chem.* 2005; 280(6):5022-5031.
53. Béraud-Dufour S, Gautier R, Albiges-Rizo C, Chardin P, Faurobert E. Krit 1 interactions with microtubules and membranes are regulated by Rap1 and integrin cytoplasmic domain associated protein-1. *FEBS J.* 2007;274(21):5518-5532.
54. Bos JL. Linking Rap to cell adhesion. *Curr Opin Cell Biol.* 2005;17(2):123-128.